HHS Public Access

Author manuscript

J Neurosci Methods. Author manuscript; available in PMC 2022 July 15.

Published in final edited form as:

J Neurosci Methods. 2021 July 15; 359: 109216. doi:10.1016/j.jneumeth.2021.109216.

Comparison of corticospinal tract integrity measures extracted from standard versus native space in chronic stroke

Allison F. Lewis[a], **Jill C. Stewart**[a,*]

[a]Department of Exercise Science, University of South Carolina, Columbia, SC 29201, USA

Abstract

Background: Fractional anisotropy (FA) and mean diffusivity (MD) are measures derived from diffusion-weighted imaging that represent the integrity of the corticospinal tract (CST) after stroke. Some studies of the motor system after stroke extract FA and MD from native space while others extract from standard space making comparison across studies challenging.

New Method: The purpose was to compare CST integrity measures extracted from standard versus native space in individuals with chronic stroke. Twenty-four individuals with stroke underwent diffusion-weighted imaging and motor impairment assessment. The spatial location of the CST was identified using four commonly utilized approaches; therefore, our results are applicable to a variety of approaches.

Results: FA extracted from standard space (FA_{std}) was significantly different from FA extracted from native space (FA_{nat}) for all four approaches; FA_{std} was greater than FA_{nat} for three approaches. The relationship between ipsilesional CST FA and UE FM was significant for all approaches and similar regardless of extraction space. MD_{std} was significantly different from MD_{nat} for most approaches, however, the directionality of the differences was not consistent.

Comparison with Existing Method(s): Our study shows that extraction space influences diffusion-based microstructural integrity values (FA and MD) of the CST in individuals with stroke, which is important when considering methods for aggregating CST integrity data across studies. The relationship between CST integrity and motor impairment appears to be robust to extraction space.

Conclusions: The differences we identified are important for comparing FA and MD values across studies that use different extraction space. Our results provide context for future meta-analyses of diffusion-based metrics of CST integrity in individuals with stroke.

*Corresponding author at: Jill Campbell Stewart, University of South Carolina, 921 Assembly Street, Room 301D, Columbia, SC 29201, USA, jcstewar@mailbox.sc.edu.

Author Statement

Allison F Lewis: Methodology, Formal analysis, Writing – Original Draft

Jill C Stewart: Conceptualization, Methodology, Validation, Resources, Project Administration, Writing – Review & Editing

Declaration of Competing Interest

The authors have no conflicts of interest to disclose.

Keywords

fractional anisotropy; mean diffusivity; stroke; diffusion-weighted imaging

1. Introduction

The corticospinal tract (CST) is a white matter tract that is important for the production and control of skilled movement. Individuals who have had a stroke can have a loss of integrity of the CST that contributes to movement dysfunction either through direct lesion to the tract or degradation due to lesion at remote sites (Arfanakis et al., 2002; Burke et al., 2014a; Lindenberg et al., 2010; Thomalla et al., 2004). One common approach to quantify the integrity of white matter tracts is through the use of diffusion-weighted imaging (DWI). Data acquired through DWI can be modeled to produce a set of values that quantify the integrity of white matter (Le Bihan and Johansen-Berg, 2012; O'Donnell and Westin, 2011). Commonly used values include fractional anisotropy (FA) and mean diffusivity (MD).

FA and MD index the integrity of white matter by quantifying water diffusion in the brain. MD quantifies the mean displacement of water diffusion, while FA represents the directional preference of water diffusion (O'Donnell and Westin, 2011; Soares et al., 2013). After stroke, the CST in the lesioned hemisphere tends to have lower FA and higher MD compared to the CST in the nonlesioned hemisphere (Burke et al., 2014a; Lindenberg et al., 2010; Stewart et al., 2017) suggesting reduced structural integrity. Many different approaches can be used to determine FA and MD in the CST with some approaches completing final data extraction from native brain space and other approaches completing final data extraction from standard brain space (Burke et al., 2014a; Cassidy et al., 2018; Lindenberg et al., 2012; Schulz et al., 2017a). Overall, the field lacks a standardized approach for the extraction of FA and MD from the CST after stroke, making comparison of data across studies challenging.

CST integrity, indexed by DWI, has been suggested as a biomarker of the motor system after stroke and potential prognostic tool to guide decisions about rehabilitative care (Boyd et al., 2017; Byblow et al., 2015; Groisser et al., 2014; Puig et al., 2017). Acquiring large imaging data sets from people with stroke is both time consuming and resource intensive. However, large data sets are needed for accurate predictive modeling and to better understand how CST integrity measures can be used to improve rehabilitative care. One option for generating larger sample sizes is aggregating smaller data sets and performing meta-analyses. Before aggregating DWI data across studies, it is important to determine how extraction space may influence the resulting CST integrity values.

Therefore, the purpose of this study was to compare diffusion-based CST integrity measures extracted from standard brain space versus native brain space in individuals with chronic stroke using four commonly used approaches for capturing the spatial location of the CST: a standard region-of-interest (ROI) based approach at the cerebral peduncle, a hand drawn ROI approach at the cerebral peduncle, a probabilistic tract approach, and a tract template approach. A secondary purpose was to investigate whether extraction space influenced the relationship between CST integrity and upper extremity motor impairment and function.

2. Materials and Methods

2.1 Participants

Structural imaging, diffusion-weighted imaging, and behavioral assessments were completed in 24 individuals in the chronic phase of stroke as part of a larger study (ClinicalTrials.gov Identifier: NCT02785419). Some participants in the current analyses were also included in a previous analysis of test-retest reliability of DWI-derived measures of CST integrity (Lewis et al., 2020). Eligibility for study participation was determined per the protocol of the larger study. Individuals were included if they were ≥18 years old, in the chronic phase of stroke recovery (>6 months post-stroke), right hand dominant prior to stroke (Oldfield, 1971) scored ≥ 19 on the Montreal Cognitive Assessment (Nasreddine et al., 2005), showed evidence of upper extremity impairment by an upper extremity Fugl-Meyer (UE FM) score (Fugl-Meyer AR, Jääskö L, Leyman I, Olsson S, 1975) < 66 and/or at least 15% deficit on the Nine Hole Peg Test (Grice et al., 2003) on the more impaired hand compared to the less impaired hand and demonstrated some movement ability as shown by an UE FM score > 30 and/or the ability to move at least one block on the Box & Blocks Test (Mathiowetz et al., 1985) with the affected upper extremity. Individuals were excluded if they had any acute medical problems, severe ideomotor apraxia as defined by a score ≤65 on the Test of Upper Limb Apraxia (Vanbellingen et al., 2010), hemispatial neglect with <52 on the BIT Star Cancellation Test (Hartman-Maeir and Katz, 1995), significant arm pain that interfered with movement, contraindications to MRI scanning (e.g., metal implants, claustrophobia), or a history of other, non-stroke related neurological disorder.

2.2 Image Acquisition

All images were acquired on a Siemens Prisma 3 Tesla MRI scanner with a 20-channel head coil at the University of South Carolina's McCausland Center for Brain Imaging. High resolution T1-weighted structural images (TR = 2250 ms, TE = 4.11 ms, 192 sagittal slices, 1 mm^3 isotropic voxels) and T2-weighted structural images (T2 = 3200 ms, TE = 567ms, 176 slices, 1 mm^3 isotropic voxels) were acquired. Diffusion-weighted images were collected using an echo-planar imaging sequence (TR = 3839 ms, TE = 71ms, 68 slices, 1.8 mm^3 isotropic voxels, 56 non-collinear directions, b = 1000 s/mm2) in two runs with reverse encoding directions (anterior to posterior and posterior to anterior); seven b0 volumes were acquired in each run.

2.3 Image Preprocessing

2.3.1 Diffusion Images—All DWI image processing was completed in FMRIB's Software Library (FSL) (FMRIB Center, Oxford, UK) using the FMRIB's Diffusion Toolbox (FDT). Volumes without diffusion weighting (b0 volumes) were extracted from both phase encoding directions, merged, and utilized to estimate susceptibility induced distortions using FSL's topup command (Andersson et al., 2003). The skull and dura were removed (Smith, 2002), and images were corrected for the eddy current-induced off-resonance fields (Andersson and Sotiropoulos, 2016). Voxelwise maps of fractional anisotropy (FA) and mean diffusivity (MD) were created using DTIFIT (Behrens et al., 2003). Images were visually inspected for quality during each step of preprocessing.

Bedposting was completed to build distributions of diffusion parameters at each voxel (Behrens et al., 2007).

2.3.2 Lesion Mask—FSL's Brain Extraction Tool was used to perform brain extraction using robust brain center estimation and thresholding to maintain inclusion of lesioned and exclude extraneous non-brain tissues (Smith, 2002). A trained researcher hand drew stroke lesion masks on the T2 structural image. All lesion masks were checked by a second, experienced researcher. The T2 lesion mask was linearly registered to the structural T1 using FSL's FLIRT, then binarized to be used as a weighting volume during registration processes. The lesion mask volume was deweighted during all linear and nonlinear registration processes (Brett et al., 2001; Schulz et al., 2017a).

2.3.3 Registration Processes

T1 Structural to Native Diffusion Space Registration: The structural T1 image was registered into native diffusion space using FSL's FLIRT and FNIRT, respectively (Jenkinson and Smith, 2001; Smith et al., 2004). The default interpolation method (trilinear) was utilized. The T1 structural image registered to native diffusion space served as the structural base for future mask drawing for the CP Hand Drawn ROI approach (Section 2.4.1) and for drawing waypoint masks and exclusion masks in the Probabilistic Tract Approach (Section 2.4.3).

Native Space to Standard Space Registration: The native space FA map was linearly then nonlinearly registered to the FMRIB FA template, which is in standard MNI space, using FSL's FLIRT and FNIRT, respectively. The default interpolation method (trilinear) was utilized. The lesion was masked out during these processes. The results of the linear and nonlinear registration steps were two nonlinear warps (native to standard; standard to native) that were applied in the approaches described in Section 2.4 (Archer et al., 2017b).

2.4 Data Extraction Approaches

Four approaches were used to extract mean FA and MD from the ipsilesional and contralesional CST from standard MNI space and each participant's native space: CP Hand Drawn ROI (Fig. 1A), CP Template ROI (Fig. 1B), Probabilistic Tract (Fig. 1C), and Tract Template (Fig. 1D). For the CP Hand Drawn ROI approach, the CP ROI was generated in native space. For the CP Template ROI approach, the CP ROI was generated in standard space. In all approaches, the final masks used for data extraction were thresholded to include voxels with an FA > 0.2. For all approaches, lesioned voxels were not included in the final masks used for data extraction.

FA ratio and FA asymmetry were calculated from the mean FA values from the ipsilesional and contralesional CST. These values represent ipsilesional tract integrity normalized to contralesional tract integrity. FA ratio values were calculated by dividing the ipsilesional CST FA value by the contralesional CST value, where a value of 1 indicates symmetrical tract integrity (FA_{ipsi}/FA_{contra}). FA asymmetry was calculated by taking the difference of the two tracts and dividing by the sum of the two tracts, where a value of zero indicates symmetrical tract integrity ($(FA_{contra} - FA_{ipsi})/(FA_{ipsi} + FA_{contra})$) (Stinear et al., 2007).

2.4.1 CP Hand Drawn ROI Approach

Standard: A CP mask was drawn in native space then transformed into standard space. To draw the mask, the T1 structural image was registered to native diffusion space. Next, the colored FA map was overlaid on the T1 structural image in native diffusion space for ROI mask drawing. A single researcher hand drew two masks (ipsilesional, contralesional) on the three contiguous axial slices (1.8 mm thick slices) that showed the largest cross-sectional area of the cerebral peduncle.(Mark et al., 2008; Schaechter et al., 2008) All masks were checked by a second researcher. The hand drawn ROI masks were nonlinearly registered to standard MNI space. FA and MD data registered to standard space were extracted from the resulting CP ROI masks

Native: A single researcher hand drew an ROI mask at the cerebral peduncle in native brain space as described above in *Standard*. FA and MD were extracted from each CP ROI mask in native space (ipsilesional, contralesional).

2.4.2 CP Template ROI Approach

Standard: The Johns Hopkins (JHU) template of the CP was used as basis for the CP template ROI (available in FSL) (Hua et al., 2008; Mori et al., 2005; Wakana et al., 2007). Five axial slices (1 mm thick slices) with the largest cross-sectional area were selected from the JHU CP template for the CP Template ROI. FA and MD data registered to standard space was extracted from the resulting CP template ROI masks.

Native: The CP Template ROI (described above in *Standard*) was nonlinearly registered to native space. FA and MD data was extracted from the resulting CP template ROI masks.

2.4.3 Probabilistic Tract Approach

Standard: Standard human motor area templates (HMATs) (Mayka et al., 2006) of primary motor cortex (M1), dorsal premotor cortex (PMd), ventral premotor cortex (PMv), supplementary motor area (SMA), pre-supplementary motor area (preSMA), and primary somatosensory cortex (S1) were used to seed probabilistic tractography, creating an individual descending probable tract from each HMAT in each hemisphere. Tractography was completed using PROBTRACKX2 in FSL (maximum number of steps=2000, step length=0.5 mm, number of samples=5000, curvature thresholds=0.2, volume fraction before subsidiary fibre volume threshold=0.01) with each HMAT as the seed region and waypoints in the posterior limb of the internal capsule and the cerebral peduncle (waycondition “AND”). The option for “Seed space is not diffusion” and “nonlinear” was selected. The respective nonlinear transforms created in Section 2.3.3 Registration Processes were added to the options for “Select Seed to diff transform” and “Select diff to seed transform”. Three exclusion masks drawn on the standard MNI brain were also included to limit extraneous fibers that crossed midline, extended into the cerebellum, or were likely part of the alternate motor pathway in the tegmentum pontis. This process resulted in six tracts per hemisphere per participant, one for each of the HMATs. Each tract was normalized by dividing the distribution by the waytotal and thresholding to include only voxels with at least 1% of total successful streamlines (Schulz et al., 2017b). The six component descending tracts for each hemisphere were combined to create a final CST tract for the ipsilesional and contralesional

hemisphere. FA and MD data registered to standard space were extracted from the resulting probabilistic CST masks.

Native: Standard human motor area templates (HMATs) of M1, PMd, PMv, SMA, preSMA, and S1 were nonlinearly registered to the individual participant's diffusion space were used to seed probabilistic tractography. Tractography was completed using PROBTRACKX2 in FSL using the same parameters as described in *Standard*. Waypoint and exclusion masks as described in *Standard* were hand drawn for each individual in native space. Each resulting probabilistic tract was normalized, thresholded, and summed to create a final CST for each hemisphere as described in *Standard*. FA and MD data were extracted from the resulting probabilistic CST masks.

2.4.5 Tract Template Approach

Standard: A standard Sensorimotor Area Tract Template (SMATT) (Archer et al., 2017b) in standard MNI space was used as the Tract Template. FA and MD data registered to standard space were extracted from the resulting CST template masks.

Native: The SMATT was nonlinearly registered from standard space to native diffusion space (see 2.3.3 Registration Processes). FA and MD data registered to standard space were extracted from the resulting probabilistic CST template masks.

2.5 Statistical Analysis

All statistical analyses were performed in SPSS 27 (IBM Corp., Armonk, NY). Data were tested for normality using Shapiro-Wilk's test and by viewing histograms. Data that did not meet assumptions for normality were analyzed using nonparametric statistics. Means and standard deviations for ipsilesional FA/MD, contralesional FA/MD, FA ratio, and FA asymmetry were calculated for data from all four approaches and each data extraction space (standard and native). FA and MD values extracted from standard space were compared to FA and MD values extracted from native space using paired *t*-tests. The mean difference was calculated by subtracting native space values from standard space values (e.g. $FA_{std} - FA_{nat}$). The mean absolute difference was calculated by taking the absolute value of the mean difference (e.g. $|FA_{std} - FA_{nat}|$). To further compare and characterize differences in standard versus native space values, the mean absolute difference was calculated as a percentage of the mean value for that approach (percent absolute difference = mean absolute difference/average of native space CST FA value and standard space CST FA value × 100). The percent absolute difference was calculated to show the relative difference between standard space and native space values compared to the overall mean for that approach, since the mean FA and MD values varied by approach.

FA and MD values from the ipsilesional CST were compared to FA and MD values from the contralesional CST using paired *t*-tests for all four approaches and both data extraction spaces (standard and native). Cohen's *d* was calculated to estimate the effect size of the difference between the ipsilesional and contralesional sides in order to characterize how extraction space influenced the magnitude of these differences. Effect sizes were interpreted as small (d=0.20), medium (d=0.50), and large (d=0.80) (Portney and Watkins, 2009).

Finally, the ipsilesional CST FA, FA ratio, and FA asymmetry from each approach and extraction space were correlated with a measure of upper extremity impairment (UE FM) and upper extremity function (Action Research Arm Test; ARAT) using Spearman's rho due to the non-normal distribution of the UE FM and ARAT scores. All paired comparisons and correlations were considered significant at $p<0.0125$ (corrected for number of approaches).

3. Results

3.1 Participants

Thirty-two participants were recruited as part of a separate clinical trial. Of these participants, 25 had structural MRI scans prior to intervention. One participant was excluded from group analyses because of poor quality of the transformation between native and standard space upon visual inspection. The final analysis included 24 participants who were on average 59.6 years old (range 35–76 years) and presented with mild to moderate upper extremity impairment (mean UE FM of 38.5, range 18–61). Participants were all in the chronic phase of stroke (mean of 34.7 months post-stroke, range 6–158 months) with variable lesion side and locations (Table 1, Fig. 2).

3.2 Comparison of Corticospinal Tract Integrity in Native versus Standard Space

FA_{nat} was significantly lower than FA_{std} for the both the ipsilesional and contralesional CST for all approaches ($p<0.0125$) except the CP Hand Drawn ROI approach. For the CP Hand Drawn ROI approach, FA_{nat} values were significantly higher than FA_{std} for the ipsilesional and contralesional CST ($p<0.001$) (Table 2). The absolute magnitude of the difference between FA_{std} and FA_{nat} ranged from 0.011 to 0.082, where the CP Hand Drawn ROI approach demonstrated the largest magnitude difference and the Tract Template approach demonstrated the smallest magnitude difference (Fig. 3). For the ipsilesional CST, the percent absolute difference in FA was 11.29% for the CP Hand Drawn ROI approach, 4.12% for the CP Template ROI approach, 6.08% for the Probabilistic Tract approach, and 3.47% for the Tract Template approach. For the contralesional CST, the percent absolute difference in FA was 13.82% for the CP Hand Drawn ROI approach, 4.09% for the CP Template ROI approach, 6.71% for the Probabilistic Tract approach, and 2.44% for the Tract Template approach.

FA ratio and asymmetry in standard space were not significantly different from FA ratio and asymmetry in native space for CP Template ROI, Probabilistic Tract, and Tract Template approaches. However, FA ratio and asymmetry in standard space were significantly different from the FA ratio and asymmetry in native space for the CP Hand Drawn approach (Table 2). The absolute magnitude of the difference between FA ratio in standard space and FA ratio in native space ranged from 0.017 to 0.039. The absolute magnitude of the difference between FA asymmetry in standard space and FA asymmetry in native space ranged from 0.009 to 0.022. For both FA ratio and asymmetry, the CP Hand Drawn ROI approach demonstrated the largest magnitude difference and the Tract Template approach demonstrated the smallest magnitude difference.

For all approaches, MD_{nat} was significantly different than MD_{std} ($p<0.0125$), except for the ipsilesional CST MD values from the CP Template ROI approach ($p=0.126$) and the Probabilistic Tract approach ($p=0.622$). MD_{nat} was not consistently higher or lower than MD_{std} across approaches (Table 2). The absolute magnitude of the difference between MD_{std} and MD_{nat} ranged from 0.007 to 0.140 × 10^{-3} mm^2/s, where the CP Hand Drawn ROI approach demonstrated the largest magnitude difference and the Probabilistic Tract and Tract Template approach demonstrated the smallest magnitude difference. For the ipsilesional CST, the percent absolute difference in MD was 8.95% for the CP Hand Drawn ROI approach, 2.22% for the CP Template ROI approach, 1.82% for the Probabilistic Tract approach, and 2.92% for the Tract Template approach. For the contralesional CST, the percent absolute difference in MD was 13.89% for the CP Hand Drawn ROI approach, 2.73% for the CP Template ROI approach, 1.24% for the Probabilistic Tract approach, and 0.91% for the Tract Template approach.

As expected, FA values for the ipsilesional CST were significantly lower than FA values for the contralesional CST ($p<0.0125$) for all four approaches and for both data extraction spaces (standard and native). MD values for the ipsilesional CST were significantly higher than MD values for the contralesional CST ($p<0.0125$) for all approaches and for both data extraction spaces, except for the CP Template ROI approach (Table 2). The effect size (Cohen's *d*) for the difference between ipsilesional CST FA and contralesional CST FA was large for all approaches. For the Tract Template approach, the effect size between ipsilesional CST FA and contralesional CST FA was slightly larger when calculated from standard space values ($d=1.92$) versus from native space values ($d=1.79$). For the Probabilistic Tract approach, the effect size calculated from standard space values ($d=1.46$) was larger than from native space values ($d=1.35$). For the CP Hand Drawn ROI approach and CP Template ROI approach, the effect size was similar regardless of extraction space (CP Hand Drawn ROI: $d=1.34$ from standard space, $d=1.32$ from native space; CP Template ROI: $d=1.11$ from standard space, $d=1.08$ from native space).

We examined the correlation between lesion volume and the absolute difference between FA_{std} and FA_{nat} to determine if lesion size impacted the differences found in FA between extraction spaces. The relationship between lesion volume and absolute difference was not significant for the CP Template ROI approach ($\rho=0.132$, $p=0.538$), the Probabilistic Tract approach ($\rho=0.128$, $p=0.552$), or the Tract Template approach ($\rho=-0.038$, $p=0.859$). The relationship between lesion volume and absolute difference was significant for the CP Hand Drawn ROI approach ($\rho=0.671$, $p<0.001$).

3.4 Relationships between Corticospinal Tract Integrity and Motor Impairment and Arm Function

FA of the ipsilesional CST was significantly correlated with upper extremity motor impairment (UE FM) for all four approaches regardless of which space the data was extracted from ($\rho=0.539$ to 0.701, $p<0.0125$) (Fig. 4, Table 3). FA ratio and asymmetry were significantly correlated with UE FM regardless of data extraction space for the CP Template ROI approach and CP Hand Drawn ROI approach. The standard space FA ratio and asymmetry for the Probabilistic Tract and Tract Template approach were significantly

correlated with UE FM. However, the native space FA ratio and asymmetry for the Probabilistic Tract approach and Tract Template did not meet criteria for significance at the corrected p value of $p<0.0125$ (Probabilistic Tract ratio and asymmetry $p=0.016$: Tract Template ratio and asymmetry $p=0.023$).

FA of the ipsilesional CST was significantly correlated with upper extremity motor function (ARAT) for three of four approaches (Table 3). FA ratio and FA asymmetry were significantly correlated ARAT score for the CP Hand Drawn ROI and CP Template ROI approach. Extraction space did not change the significance of the relationship between FA and upper extremity motor function as measured by the ARAT for any of the approaches.

4. Discussion

This study examined diffusion-based CST integrity measures (FA and MD) extracted from standard brain space versus native brain space in individuals with chronic stroke using four commonly used approaches for capturing the spatial location of the CST. Our study showed that FA and MD values extracted from standard space are significantly different than FA and MD values extracted from native space when using the same approach for identifying and capturing the CST. FA_{std} was higher than FA_{nat} for all approaches except for the CP Hand Drawn ROI approach. MD_{std} was significantly different than MD_{nat} for all approaches, however, the directionality of this difference was not consistent. The reason for this difference in directionality is unclear but could be due to the nature of the calculation of MD versus FA, where MD is a mean of the eigenvalues and FA is a ratio of the eigenvalues. Importantly, the relationship between the ipsilesional CST FA value and motor impairment (UE FM) and motor function (ARAT) was similar regardless of extraction space. The differences in FA and MD based on extraction space identified here may impact the comparison of results across studies and highlight the need for standards of reporting diffusion data including the space from which final data extraction was completed.

The structural integrity of the CST has been suggested as a biomarker of the motor system after stroke (Boyd et al., 2017; Puig et al., 2017). Diffusion-based measures of CST integrity (e.g. FA, MD) are commonly reported in studies of motor status and motor recovery after stroke. However, there is no gold standard for the extraction and reporting of these measures. Some studies extract FA and MD in native diffusion space while other studies extract FA and MD from standard space; some studies do not clearly report the space from which the data was extracted (Borich et al., 2012; Burke et al., 2014a; Cassidy et al., 2018; Lindenberg et al., 2012; Schulz et al., 2017b). FA and MD data can serve several purposes in the study of the motor recovery after stroke including to describe the study population (Stewart et al., 2016), relate white matter integrity to measures of motor behavior (e.g. correlations between UE FM and CST FA) (Burke et al., 2014b), and compare the integrity of white matter between the lesioned and nonlesioned hemispheres (Lindenberg et al., 2010). The interpretation of and comparison between studies that include FA and MD after stroke could be impacted by the space used for data extraction.

First, our results inform how two studies that use different extraction spaces can be compared or interpreted when using FA and MD to describe the study population. The

absolute differences, mean absolute differences, and percent differences that we calculated will allow for assessment of how similar two populations are across studies that use different extraction spaces to measure CST integrity. For example, if Study A utilized the Tract Template approach in standard space and Study B used the Tract Template approach in native space, we would expect that the mean FA value for the population in Study A to be about 3.47% higher than the mean FA values for the population in Study B. If differences are larger or smaller, this may indicate true differences between the populations in the two studies (e.g. more degradation of the CST in one population) not associated with different extraction spaces. In this case, methodology between studies would have to be closely assessed and compared to identify if other aspects of the methods (e.g. variations in normalization processes) might contribute to differences. Other characteristics of the study population, like age, time since stroke, and severity might also be considered as factors contributing to differences in FA values between studies.

Second, our results suggest that extraction space is not a significant consideration when interpreting or comparing studies that relate CST FA to motor impairment and motor function of the upper extremity, since extraction space did not impact these brain-behavior relationships. If two studies utilized the same approach (e.g. Tract Template) but extracted data from different space (i.e. standard space vs. native space), we would expect the correlations between CST FA and UE FM to be significant and similar for both studies. The same would be true for correlations between CST FA and ARAT. However, these findings may be specific to relationships between CST FA from individuals in the chronic phase of stroke with mild to moderate upper extremity impairment and these behavioral measures (UE FM and ARAT); differences in brain-behavior relationship based on extraction space may exist when FA is related to other measures of motor function, when other white matter tracts are investigated, or when examining individuals in the acute phase of stroke or those with more severe impairment.

Third, when comparing the integrity of white matter between the lesioned and nonlesioned hemisphere, our results suggest that differences between FA and MD in the lesioned and nonlesioned hemispheres will be influenced by extraction space and approach used. Researchers that employ the Probabilistic Tract or Tract Template approach to measure CST integrity would expect to find larger differences between hemispheres if extracting data from standard space versus native space. For example, a study that used the Tract Template approach in standard space (Cohen's d=1.92) would be expected to show larger differences between the lesioned and nonlesioned hemisphere CST FA than a study that utilized the Tract Template approach in native space (Cohen's d=1.79). It should be noted that this relationship may differ by approach. The magnitude of the effect size varied between approaches from d=1.08 (native space CP Template ROI approach) to d=1.92 (standard space Tract Template approach).

Finally, our results have implications for the pooling or aggregating of diffusion-based CST integrity measures in individuals with mild to moderate arm motor impairment due to chronic stroke. Pooling data across many sites may be especially valuable in studying recovery after stroke since acquiring large datasets with brain imaging can be costly. However, researchers often utilize different approaches and extraction spaces to evaluate

CST integrity (Archer et al., 2017a; Feldman et al., 2018; Kim et al., 2018; Schulz et al., 2017b). A common criticism of meta-analyses is that researchers "mix apples and oranges" and include data from a variety of studies despite important differences (Borenstein et al., 2009). Since our study showed significant differences between standard space data ("apple data") and native space data ("orange data"), statistical approaches should be adjusted to account for these differences by harmonizing the data. Harmonization refers to mathematical approaches used to adjust the data to account for differences in site, scanner, or protocol during meta-analysis (site-aggregated statistical data like effect sizes) and mega-analysis (individual subject data). While there are not any published meta-analyses of DTI data from individuals with stroke, there are many published meta- and mega-analyses in other clinical populations that may serve as useful models for how to apply harmonization methods for future analyses in chronic stroke (Favre et al., 2019; Kelly et al., 2018; Koshiyama et al., 2020; Radua et al., 2020).

While the purpose of this study was to compare data extracted from native versus standard space, it is important to consider the influence of different approaches for identifying the spatial location of the CST on the data. In a previous analysis, our group found differences in the range of FA_{nat} values when using an ROI approach versus full tract approaches (Probabilistic Tract and Tract Template). The ROI approach resulted in higher mean FA value compared to full tract approaches (Lewis et al., 2020). The current study replicates these findings in standard space data with FA_{std} values showing higher mean values in the CP Template ROI approach than in the Probabilistic Tract and Tract Template approach. These results further highlight how the approach selected for identifying the spatial location of the CST can influence resulting CST integrity values. Harmonization approaches should be used to account for these differences in measurement when pooling diffusion-based CST integrity data from studies that utilized different approaches for identifying the spatial location of the CST.

Each extraction space has advantages and disadvantages. In general, extracting FA and MD from native space may reduce the impacts of normalization processes on the raw data. Difficulties with normalization in lesioned brains have been documented (Kim et al., 2018), though we believe our normalization process accounted for lesions well based on detailed visual inspection and the finding that lesion size was generally not correlated with the differences between native and standard space FA values. Extracting FA and MD from standard space is advantageous in that the location of the CST can be standardized across all individuals by using standard space templates. Given these advantages, data extraction from standard space may be well suited for multisite investigations with large numbers of participants. Further, each approach for identifying the spatial location of the CST has advantages and disadvantages. Some approaches require more technical expertise than others (e.g. the Probabilistic Tract approach versus the Hand Drawn ROI approach) while some approaches have higher test-retest reliability than others (e.g. the Tract Template and Probabilistic Tract approach has higher reliability than the Hand Drawn CP ROI approach) (Lewis et al., 2020). All of these factors should be weighed in determining the optimal approach for determining CST integrity in each research study.

Our methods include four commonly utilized approaches for measuring CST FA and MD after stroke. The inclusion of four approaches enhances the applicability of our findings. As such, the results presented may be utilized for interpretation of data across research studies that employ a variety of methods and approaches for extraction of CST FA and MD. In the current study, we utilized two different CP ROI approaches. The first approach required that hand drawn ROIs be generated in native space, and the other utilized a standard space template as would be customary for ROI data extraction from standard space. For the purpose of comparisons, we applied transformations to the hand drawn and template CP ROI masks to allow us to make direct comparisons between native and standard space data. However, we realize that transforming hand drawn masks to standard space for data extraction would not necessarily be a practical approach for extracting CST integrity data.

The aim of the current study was to examine the difference in CST FA extracted from native versus standard space after stroke. Overall, this study is a first step in understanding how variations in methods might impact resulting CST integrity data in individuals with chronic stroke which may serve as a starting point for future studies. We selected commonly utilized approaches for identifying the spatial location of the CST and chose a similar registration process as was applied to create the CST template that we utilized in the Tract Template Approach (a combination of FSL's FLIRT/FNIRT using trilinear interpolation) (Archer et al., 2017b). We acknowledge that this is only one approach to registration using a single interpolation technique. Different registration approaches and/or interpolation techniques may not result in the same relationships between native and standard space FA values found in the current study. Similarly, probabilistic tractography approaches can vary between research studies depending on thresholding, region of interest placement for seeding tracts, region of interest placement for waypointing tracts, and how the diffusion data is modeled in the bedposting process. These decisions may impact the spatial location of the final tract and/or the data contained in the voxels captured by the final tract. Future research should aim to perform similar analyses as performed here to quantify the impact of these other variations in the measurement of CST integrity after stroke.

Our participants presented with variable lesion size and location which contributes to the generalizability of our findings. However, the difference between values extracted from native versus standard space could be influenced by lesion size since some approaches relied heavily on transformation processes (i.e. the Tract Template Approach) and difficulties with transformation processes in lesioned brains have been documented (Kim et al., 2018). We aimed to limit these effects by masking out lesions during the transformation processes. Additionally, lesion volume did not correlate with differences between FA_{std} and FA_{nat} for three of the four approaches suggesting lesion volume was not a significant driver of the differences between standard and native space values. Finally, our results are based on individuals in the chronic phase of stroke (>6 months post) with mostly mild to moderate upper extremity impairment and may not be useful for interpreting data from individuals in the acute or subacute phase of recovery or from individuals with more severe impairment. Previous research indicates that severity may impact brain-behavior relationships (Feldman et al., 2018; Quinlan et al., 2018; Stewart et al., 2017). It is possible that the relationships between CST $FA_{nat/std}$ and UEFM and CST $FA_{nat/std}$ and ARAT would also be different in a population with more severe impairment.

5. Conclusion

Measures of CST integrity from diffusion-weighted imaging (FA, MD) extracted from standard space were different than the same measures extracted from native space. FA_{std} was larger than FA_{nat} for all approaches, except for the CP Hand Drawn ROI approach. The direction of the differences did not follow the same pattern for MD, where MD_{std} was not consistently higher or lower than MD_{nat}. However, extraction space did not influence the relationship between FA and motor impairment as measured by the UE FM. Our results provide context for interpreting CST integrity values across studies that utilize different methods for measuring FA and MD and highlights important considerations for meta-analyses on studies of brain structure after stroke. Research studies that report CST integrity from individuals with stroke should be clear about how FA and MD were measured by including detailed information about their approach and the space the data was extracted from (standard versus native). The field of neuroimaging and stroke recovery would benefit from standards and guidelines for reporting data in research publications as well as consensus on accepted methodologies for measuring white matter integrity.

Acknowledgements

This work was supported by grants from the National Institutes of Health (R03 HD087481) and the American Heart Association (20PRE35180106 and 15SDG24970011). The funding sources did not influence or play a role in the study design, interpretation of the data, or in the writing of this manuscript. The authors thank Olivia Lockhart, Makenzie Myers, and Jenny Heiser for their assistance with some data processing steps.

References

Andersson JLR, Skare S, Ashburner J, 2003. How to correct susceptibility distortions in spin-echo echo-planar images: Application to diffusion tensor imaging. Neuroimage 20, 870–888. 10.1016/S1053-8119(03)00336-7 [PubMed: 14568458]

Andersson JLR, Sotiropoulos SN, 2016. An integrated approach to correction for off-resonance effects and subject movement in diffusion MR imaging. Neuroimage 125, 1063–1078. 10.1016/j.neuroimage.2015.10.019 [PubMed: 26481672]

Archer DB, Patten C, Coombes SA, 2017a. Free-water and free-water corrected fractional anisotropy in primary and premotor corticospinal tracts in chronic stroke. Hum. Brain Mapp 38, 4546–4562. 10.1002/hbm.23681 [PubMed: 28590584]

Archer DB, Vaillancourt DE, Coombes SA, 2017b. A Template and Probabilistic Atlas of the Human Sensorimotor Tracts using Diffusion MRI. Cereb. Cortex 28, 1–15. 10.1093/cercor/bhx066

Arfanakis K, Haughton VM, Carew JD, Rogers BP, Dempsey RJ, Meyerand ME, 2002. Diffusion tensor MR imaging in diffuse axonal injury. Am. J. Neuroradiol 23, 794–802. 10.3174/ajnr.a0970 [PubMed: 12006280]

Behrens TEJ, Berg HJ, Jbabdi S, Rushworth MFS, Woolrich MW, 2007. Probabilistic diffusion tractography with multiple fibre orientations: What can we gain? Neuroimage 34, 144–155. 10.1016/j.neuroimage.2006.09.018 [PubMed: 17070705]

Behrens TJ, Woolrich MW, Jenkinson M, Johansen-Berg H, Nunes RG, Clare S, Matthews PM, Brady JM, Smith SM, 2003. Characterization and Propagation of Uncertainty in Diffusion-Weighted MR Imaging. Magn. Reson. Med 50, 1077–1088. 10.1002/mrm.10609 [PubMed: 14587019]

Borenstein M, Hedges LV, Higgins JPT, Rothstein HR, 2009. Introduction to Meta-Analysis, Introduction to Meta-Analysis. 10.1002/9780470743386

Borich MR, Wadden KP, Boyd LA, 2012. Establishing the reproducibility of two approaches to quantify white matter tract integrity in stroke. Neuroimage 59, 2393–2400. 10.1016/j.neuroimage.2011.09.009 [PubMed: 21945470]

Boyd LA, Hayward KS, Ward NS, Stinear CM, Rosso C, Fisher RJ, Carter AR, Leff AP, Copland DA, Carey LM, Cohen LG, Basso DM, Maguire JM, Cramer SC, 2017. Biomarkers of Stroke Recovery: Consensus-Based Core Recommendations from the Stroke Recovery and Rehabilitation Roundtable*. Neurorehabil. Neural Repair 31, 864–876. 10.1177/1545968317732680 [PubMed: 29233071]

Brett M, Leff AP, Rorden C, Ashburner J, 2001. Spatial normalization of brain images with focal lesions using cost function masking. Neuroimage 14, 486–500. 10.1006/nimg.2001.0845 [PubMed: 11467921]

Burke E, Dodakian L, See J, McKenzie A, Riley JD, Le V, Cramer SC, 2014a. A multimodal approach to understanding motor impairment and disability after stroke. J. Neurol 261, 1178–1186. 10.1007/s00415-014-7341-8 [PubMed: 24728337]

Burke E, Dodakian L, See J, McKenzie A, Riley JD, Le V, Cramer SC, 2014b. A multimodal approach to understanding motor impairment and disability after stroke. J. Neurol 261, 1178–1186. 10.1007/s00415-014-7341-8 [PubMed: 24728337]

Byblow WD, Stinear CM, Barber PA, Petoe MA, Ackerley SJ, 2015. Proportional recovery after stroke depends on corticomotor integrity. Ann. Neurol 78, 848–859. 10.1002/ana.24472 [PubMed: 26150318]

Cassidy JM, Tran G, Quinlan EB, Cramer SC, 2018. Neuroimaging identifies patients most likely to respond to a restorative stroke therapy. Stroke 49, 433–438. 10.1161/STROKEAHA.117.018844 [PubMed: 29321336]

Favre P, Pauling M, Stout J, Hozer F, Sarrazin S, Abé C, Alda M, Alloza C, Alonso-Lana S, Andreassen OA, Baune BT, Benedetti F, Busatto GF, Canales-Rodríguez EJ, Caseras X, Chaim-Avancini TM, Ching CRK, Dannlowski U, Deppe M, Eyler LT, Fatjo-Vilas M, Foley SF, Grotegerd D, Hajek T, Haukvik UK, Howells FM, Jahanshad N, Kugel H, Lagerberg TV, Lawrie SM, Linke JO, McIntosh A, Melloni EMT, Mitchell PB, Polosan M, Pomarol-Clotet E, Repple J, Roberts G, Roos A, Rosa PGP, Salvador R, Sarró S, Schofield PR, Serpa MH, Sim K, Stein DJ, Sussmann JE, Temmingh HS, Thompson PM, Verdolini N, Vieta E, Wessa M, Whalley HC, Zanetti MV, Leboyer M, Mangin JF, Henry C, Duchesnay E, Houenou J, 2019. Widespread white matter microstructural abnormalities in bipolar disorder: evidence from mega- and meta-analyses across 3033 individuals. Neuropsychopharmacology 44, 2285–2293. 10.1038/s41386-019-0485-6 [PubMed: 31434102]

Feldman SJ, Boyd LA, Neva JL, Peters S, Hayward KS, 2018. Extraction of corticospinal tract microstructural properties in chronic stroke. J. Neurosci. Methods 301, 34–42. 10.1016/j.jneumeth.2018.03.001 [PubMed: 29522781]

Fugl-Meyer AR, Jääskö L, Leyman I, Olsson S, S. S, 1975. The post-stroke hemiplegic patient. 1. a method for evaluation of physical performance. Scand. J. Rehabil. Med 7, 13–31. 10.1038/35081184 [PubMed: 1135616]

Grice KO, Vogel KA, Le V, Mitchell A, Muniz S, Vollmer MA, 2003. Adult norms for a commercially available nine hole peg test for finger dexterity. Am. J. Occup. Ther 57, 570–573. 10.5014/ajot.57.5.570 [PubMed: 14527120]

Groisser BN, Copen WA, Singhal AB, Hirai KK, Schaechter JD, 2014. Corticospinal tract diffusion abnormalities early after stroke predict motor outcome. Neurorehabil. Neural Repair 28, 751–760. 10.1177/1545968314521896 [PubMed: 24519021]

Hartman-Maeir A, Katz N, 1995. Validity of the Behavioral Inattention Test (BIT): relationships with functional tasks. Am. J. Occup. Ther 49, 507–516. 10.5014/ajot.49.6.507 [PubMed: 7645663]

Hua K, Zhang J, Wakana S, Jiang H, Li X, Reich DS, Calabresi PA, Pekar JJ, van Zijl PCM, Mori S, 2008. Tract probability maps in stereotaxic spaces: Analyses of white matter anatomy and tract-specific quantification. Neuroimage 10.1016/j.neuroimage.2007.07.053

Jenkinson M, Smith S, 2001. A global optimisation method for robust affine registration of brain images. Med. Image Anal 5, 143–156. 10.1016/S1361-8415(01)00036-6 [PubMed: 11516708]

Kelly S, Jahanshad N, Zalesky A, Kochunov P, Agartz I, Alloza C, Andreassen OA, Arango C, Banaj N, Bouix S, Bousman CA, Brouwer RM, Bruggemann J, Bustillo J, Cahn W, Calhoun V, Cannon D, Carr V, Catts S, Chen J, Chen JX, Chen X, Chiapponi C, Cho KK, Ciullo V, Corvin AS, Crespo-Facorro B, Cropley V, De Rossi P, Diaz-Caneja CM, Dickie EW, Ehrlich S, Fan FM, Faskowitz J, Fatouros-Bergman H, Flyckt L, Ford JM, Fouche JP, Fukunaga M, Gill M, Glahn DC,

Gollub R, Goudzwaard ED, Guo H, Gur RE, Gur RC, Gurholt TP, Hashimoto R, Hatton SN, Henskens FA, Hibar DP, Hickie IB, Hong LE, Horacek J, Howells FM, Hulshoff Pol HE, Hyde CL, Isaev D, Jablensky A, Jansen PR, Janssen J, Jönsson EG, Jung LA, Kahn RS, Kikinis Z, Liu K, Klauser P, Knöchel C, Kubicki M, Lagopoulos J, Langen C, Lawrie S, Lenroot RK, Lim KO, Lopez-Jaramillo C, Lyall A, Magnotta V, Mandl RCW, Mathalon DH, McCarley RW, McCarthy-Jones S, McDonald C, McEwen S, McIntosh A, Melicher T, Mesholam-Gately RI, Michie PT, Mowry B, Mueller BA, Newell DT, O'Donnell P, Oertel-Knöchel V, Oestreich L, Paciga SA, Pantelis C, Pasternak O, Pearlson G, Pellicano GR, Pereira A, Pineda Zapata J, Piras F, Potkin SG, Preda A, Rasser PE, Roalf DR, Roiz R, Roos A, Rotenberg D, Satterthwaite TD, Savadjiev P, Schall U, Scott RJ, Seal ML, Seidman LJ, Shannon Weickert C, Whelan CD, Shenton ME, Kwon JS, Spalletta G, Spaniel F, Sprooten E, Stäblein M, Stein DJ, Sundram S, Tan Y, Tan S, Tang S, Temmingh HS, Westlye LT, Tønnesen S, Tordesillas-Gutierrez D, Doan NT, Vaidya J, Van Haren NEM, Vargas CD, Vecchio D, Velakoulis D, Voineskos A, Voyvodic JQ, Wang Z, Wan P, Wei D, Weickert TW, Whalley H, White T, Whitford TJ, Wojcik JD, Xiang H, Xie Z, Yamamori H, Yang F, Yao N, Zhang G, Zhao J, Van Erp TGM, Turner J, Thompson PM, Donohoe G, 2018. Widespread white matter microstructural differences in schizophrenia across 4322 individuals: Results from the ENIGMA Schizophrenia DTI Working Group. Mol. Psychiatry 23, 1261–1269. 10.1038/mp.2017.170 [PubMed: 29038599]

Kim B, Fisher BE, Schweighofer N, Leahy RM, Haldar JP, Choi S, Kay DB, Gordon J, Winstein CJ, 2018. A comparison of seven different DTI-derived estimates of corticospinal tract structural characteristics in chronic stroke survivors. J. Neurosci. Methods 304, 66–75. 10.1016/j.jneumeth.2018.04.010 [PubMed: 29684462]

Koshiyama D, Fukunaga M, Okada N, Morita K, Nemoto K, Usui K, Yamamori H, Yasuda Y, Fujimoto M, Kudo N, Azechi H, Watanabe Y, Hashimoto N, Narita H, Kusumi I, Ohi K, Shimada T, Kataoka Y, Yamamoto M, Ozaki N, Okada G, Okamoto Y, Harada K, Matsuo K, Yamasue H, Abe O, Hashimoto Ryuichiro, Takahashi T, Hori T, Nakataki M, Onitsuka T, Holleran L, Jahanshad N, van Erp TGM, Turner J, Donohoe G, Thompson PM, Kasai K, Hashimoto Ryota, 2020. White matter microstructural alterations across four major psychiatric disorders: mega-analysis study in 2937 individuals. Mol. Psychiatry 25, 883–895. 10.1038/s41380-019-0553-7 [PubMed: 31780770]

Le Bihan D, Johansen-Berg H, 2012. Diffusion MRI at 25: Exploring brain tissue structure and function. Neuroimage 61, 324–341. 10.1016/j.neuroimage.2011.11.006 [PubMed: 22120012]

Lewis AF, Myers M, Heiser J, Kolar M, Baird JF, Stewart JC, 2020. Test–retest reliability and minimal detectable change of corticospinal tract integrity in chronic stroke. Hum. Brain Mapp 41, 2514–2526. 10.1002/hbm.24961 [PubMed: 32090440]

Lindenberg R, Renga V, Zhu LL, Betzler F, Alsop D, Schlaug G, 2010. Structural integrity of corticospinal motor fibers predicts motor impairment in chronic stroke. Neurology 74, 280–7. 10.1212/WNL.0b013e3181ccc6d9 [PubMed: 20101033]

Lindenberg R, Zhu LL, Rüber T, Schlaug G, 2012. Predicting functional motor potential in chronic stroke patients using diffusion tensor imaging. Hum. Brain Mapp 33, 1040–1051. 10.1002/hbm.21266 [PubMed: 21538700]

Mark VW, Taub E, Perkins C, Gauthier LV, Uswatte G, Ogorek J, 2008. Poststroke cerebral peduncular atrophy correlates with a measure of corticospinal tract injury in the cerebral hemisphere. Am. J. Neuroradiol 29, 354–358. 10.3174/ajnr.A0811 [PubMed: 18024577]

Mathiowetz V, Federman S, Wiemer D, 1985. Box and Block Test of Manual Dexterity. Can. J. Occup. Ther 52, 241–245.

Mayka MA, Corcos DM, Leurgans SE, Vaillancourt DE, 2006. Three-dimensional locations and boundaries of motor and premotor cortices as defined by functional brain imaging: A meta-analysis. Neuroimage 31, 1453–1474. 10.1016/j.neuroimage.2006.02.004 [PubMed: 16571375]

Mori S, Wakana S, Nagae-Poetscher L, van Zijl P, 2005. MRI atlas of human white matter. Elsevier, Amsterdam, The Netherlands.

Nasreddine ZS, Phillips NA, Bédirian V, Charbonneau S, Whitehead V, Collin I, Cummings JL, Chertkow H, 2005. The Montreal Cognitive Assessment, MoCA: a brief screening tool for mild cognitive impairment. J. Am. Geriatr. Soc 53, 695–699. 10.1111/j.1532-5415.2005.53221.x [PubMed: 15817019]

O'Donnell LJ, Westin CF, 2011. An introduction to diffusion tensor image analysis. Neurosurg. Clin. N. Am 22, 185–196. 10.1016/j.nec.2010.12.004 [PubMed: 21435570]

Oldfield RC, 1971. The assessment and analysis of handedness: The Edinburgh inventory. Neuropsychologia 9, 97–113. 10.1016/0028-3932(71)90067-4 [PubMed: 5146491]

Portney L, Watkins M, 2009. Foundations of Clinical Research: Applications to Practice, Third. ed Prentice Hall.

Puig J, Blasco G, Schlaug G, Stinear CM, Daunis-i-Estadella P, Biarnes C, Figueras J, Serena J, Hernández-Pérez M, Alberich-Bayarri A, Castellanos M, Liebeskind DS, Demchuk AM, Menon BK, Thomalla G, Nael K, Wintermark M, Pedraza S, 2017. Diffusion tensor imaging as a prognostic biomarker for motor recovery and rehabilitation after stroke. Neuroradiology. 10.1007/s00234-017-1816-0

Quinlan EB, Dodakian L, See J, McKenzie A, Stewart JC, Cramer SC, 2018. Biomarkers of rehabilitation therapy vary according to stroke severity. Neural Plast. 10.1155/2018/9867196

Radua J, Vieta E, Shinohara R, Kochunov P, Quidé Y, Green MJ, Weickert CS, Weickert T, Bruggemann J, Kircher T, Nenadić I, Cairns MJ, Seal M, Schall U, Henskens F, Fullerton JM, Mowry B, Pantelis C, Lenroot R, Cropley V, Loughland C, Scott R, Wolf D, Satterthwaite TD, Tan Y, Sim K, Piras Fabrizio, Spalletta G, Banaj N, Pomarol-Clotet E, Solanes A, Albajes-Eizagirre A, Canales-Rodríguez EJ, Sarro S, Di Giorgio A, Bertolino A, Stäblein M, Oertel V, Knöchel C, Borgwardt S, du Plessis S, Yun JY, Kwon JS, Dannlowski U, Hahn T, Grotegerd D, Alloza C, Arango C, Janssen J, Díaz-Caneja C, Jiang W, Calhoun V, Ehrlich S, Yang K, Cascella NG, Takayanagi Y, Sawa A, Tomyshev A, Lebedeva I, Kaleda V, Kirschner M, Hoschl C, Tomecek D, Skoch A, van Amelsvoort T, Bakker G, James A, Preda A, Weideman A, Stein DJ, Howells F, Uhlmann A, Temmingh H, López-Jaramillo C, Díaz-Zuluaga A, Fortea L, Martinez-Heras E, Solana E, Llufriu S, Jahanshad N, Thompson P, Turner J, van Erp T, Glahn D, Pearlson G, Hong E, Krug A, Carr V, Tooney P, Cooper G, Rasser P, Michie P, Catts S, Gur Raquel, Gur Ruben, Yang F, Fan F, Chen J, Guo H, Tan S, Wang Z, Xiang H, Piras Federica, Assogna F, Salvador R, McKenna P, Bonvino A, King M, Kaiser S, Nguyen D, Pineda-Zapata J, 2020. Increased power by harmonizing structural MRI site differences with the ComBat batch adjustment method in ENIGMA. Neuroimage 218. 10.1016/j.neuroimage.2020.116956

Schaechter JD, Perdue KL, Wang R, 2008. Structural damage to the corticospinal tract correlates with bilateral sensorimotor cortex reorganization in stroke patients. Neuroimage 39, 1370–1382. 10.1016/j.neuroimage.2007.09.071 [PubMed: 18024157]

Schulz R, Park E, Lee J, Chang WH, Lee A, Kim YH, Hummel FC, 2017a. Interactions between the corticospinal tract and premotor-motor pathways for residual motor output after stroke. Stroke 48, 2805–2811. 10.1161/STROKEAHA.117.016834 [PubMed: 28904231]

Schulz R, Park E, Lee J, Chang WH, Lee A, Kim YH, Hummel FC, 2017b. Synergistic but independent: The role of corticospinal and alternate motor fibers for residual motor output after stroke. NeuroImage Clin. 15, 118–124. 10.1016/j.nicl.2017.04.016 [PubMed: 28516034]

Smith SM, 2002. Fast robust automated brain extraction. Hum. Brain Mapp 17, 143–155. 10.1002/hbm.10062 [PubMed: 12391568]

Smith SM, Jenkinson M, Woolrich MW, Beckmann CF, Behrens TEJ, Johansen-Berg H, Bannister PR, De Luca M, Drobnjak I, Flitney DE, Niazy RK, Saunders J, Vickers J, Zhang Y, De Stefano N, Brady JM, Matthews PM, 2004. Advances in functional and structural MR image analysis and implementation as FSL. Neuroimage 23, S208–S219. 10.1016/j.neuroimage.2004.07.051 [PubMed: 15501092]

Soares JM, Marques P, Alves V, Sousa N, 2013. A hitchhiker's guide to diffusion tensor imaging. Front. Neurosci 7. 10.3389/fnins.2013.00031

Stewart JC, Dewanjee P, Shariff U, Cramer SC, 2016. Dorsal premotor activity and connectivity relate to action selection performance after stroke. Hum. Brain Mapp 37, 1816–1830. 10.1002/hbm.23138 [PubMed: 26876608]

Stewart JC, Dewanjee P, Tran G, Quinlan EB, Dodakian L, McKenzie A, See J, Cramer SC, 2017. Role of corpus callosum integrity in arm function differs based on motor severity after stroke. NeuroImage Clin. 14, 641–647. 10.1016/j.nicl.2017.02.023 [PubMed: 28348955]

Stinear CM, Barber PA, Smale PR, Coxon JP, Fleming MK, Byblow WD, 2007. Functional potential in chronic stroke patients depends on corticospinal tract integrity. Brain 130, 170–180. 10.1093/brain/awl333 [PubMed: 17148468]

Thomalla G, Glauche V, Koch MA, Beaulieu C, Weiller C, Röther J, 2004. Diffusion tensor imaging detects early Wallerian degeneration of the pyramidal tract after ischemic stroke. Neuroimage 22, 1767–1774. 10.1016/j.neuroimage.2004.03.041 [PubMed: 15275932]

Vanbellingen T, Kersten B, Van Hemelrijk B, Van De Winckel A, Bertschi M, Müri R, De Weerdt W, Bohlhalter S, 2010. Comprehensive assessment of gesture production: A new test of upper limb apraxia (TULIA). Eur. J. Neurol 17, 59–66. 10.1111/j.1468-1331.2009.02741.x [PubMed: 19614961]

Wakana S, Caprihan A, Panzenboeck MM, Fallon JH, Perry M, Gollub RL, Hua K, Zhang J, Jiang H, Dubey P, Blitz A, van Zijl P, Mori S, 2007. Reproducibility of quantitative tractography methods applied to cerebral white matter. Neuroimage 36, 630–644. 10.1016/j.neuroimage.2007.02.049 [PubMed: 17481925]

Highlights

- Corticospinal tract integrity is an important biomarker of the motor system in stroke.
- Diffusion imaging-based measures of integrity differed when extracted from standard versus native space.
- Corticospinal tract integrity related to motor impairment regardless of extraction space.
- Extraction space should be considered when comparing measures of corticospinal tract integrity across studies.

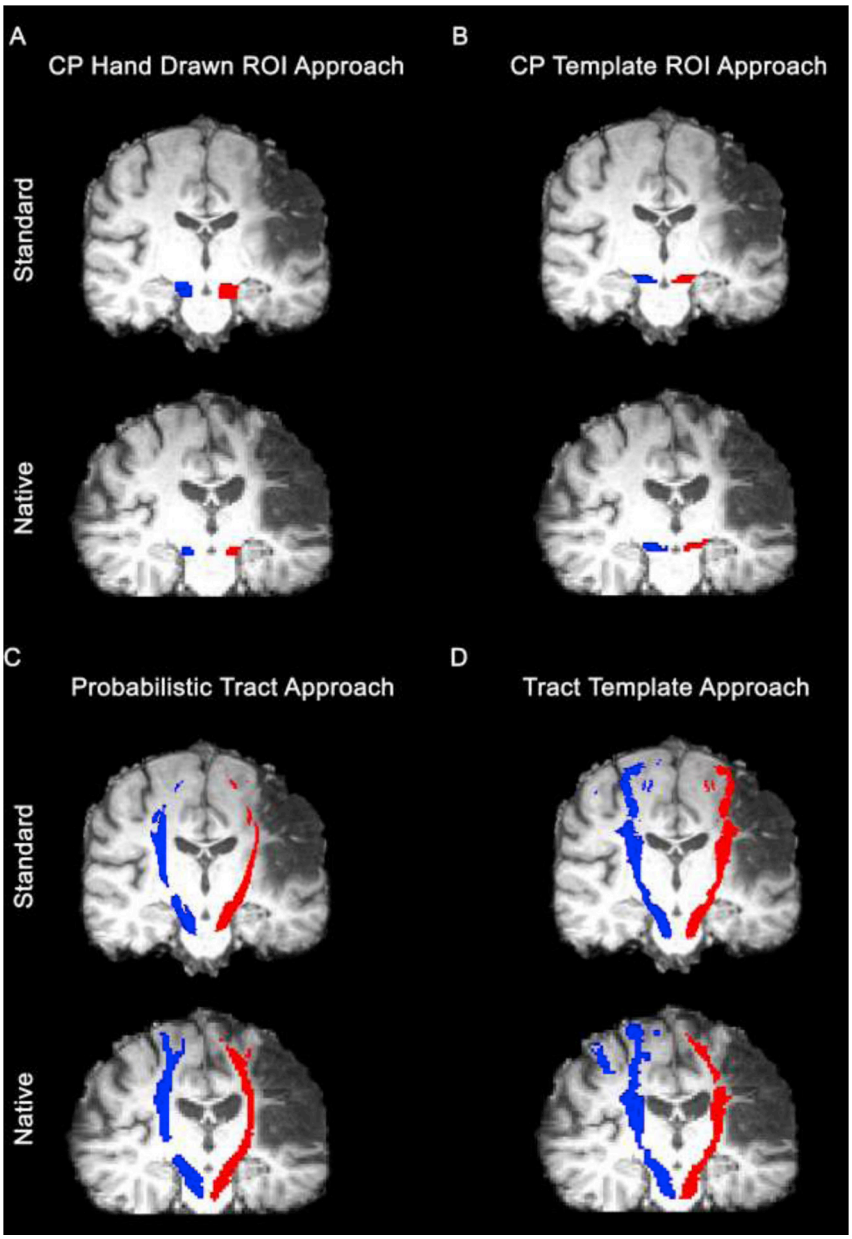

Figure 1:
Visualization of final corticospinal tract (CST) masks for a single participant for each approach: A) CP Hand Drawn ROI approach, B) CP Template ROI approach, C) Probabilistic Tract, and D) Tract Template approach. The red masks represent the spatial location of the ipsilesional CST. The blue masks represent the spatial location of the contralesional CST. CP = cerebral peduncle; ROI = region of interest

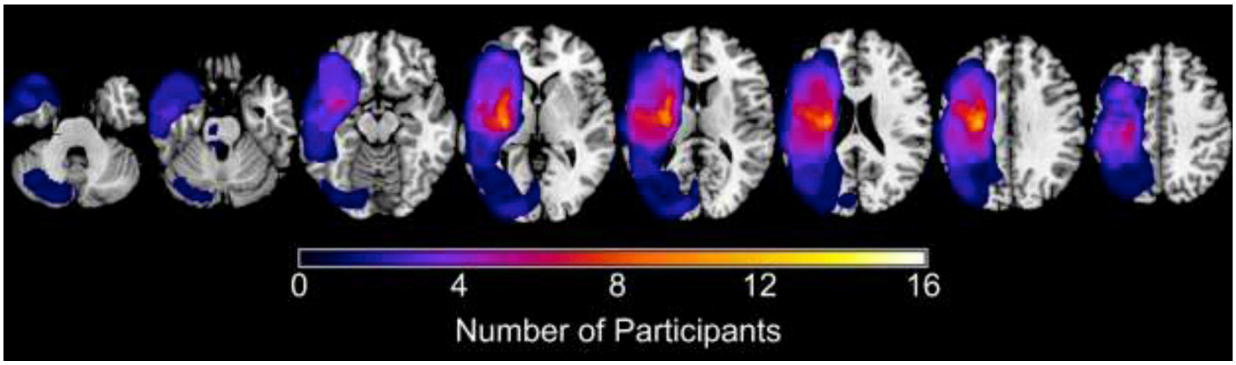

Figure 2:

Summary mask of participants' stroke lesions created in MRIcron (www.mccauslandcenter.sc.edu/micro/mricron/), where the coloration indicates the number of participants with a stroke in that region. Stroke lesions in the right hemisphere were flipped to the left hemisphere.

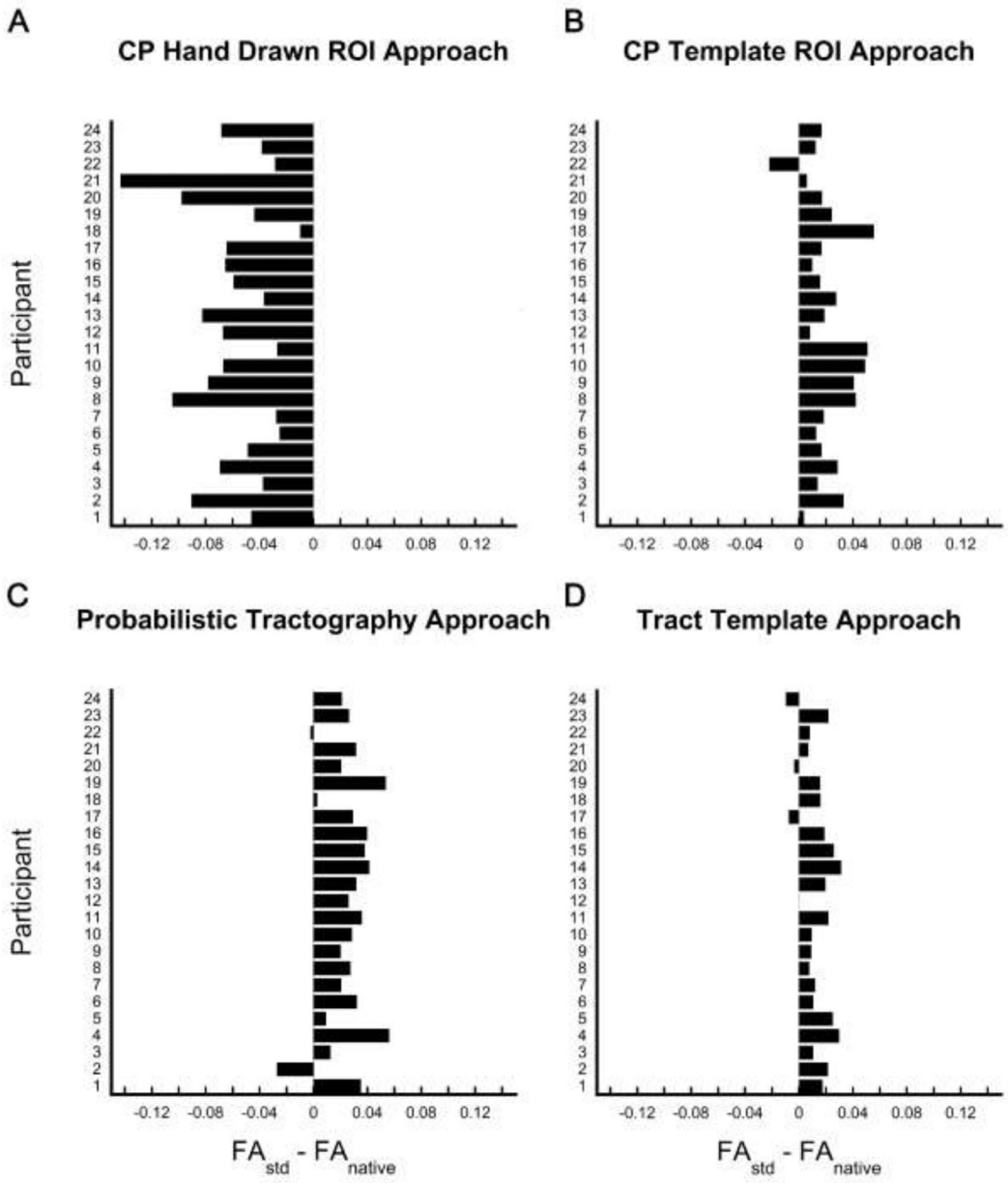

Figure 3:

Bar plots indicating the difference between corticospinal tract (CST) fractional anisotropy extracted from standard space (FA_{std}) and fractional anisotropy extracted from native space (FA_{native}) by individual participant. Bars that fall to the right of zero indicate the FA_{std} was greater than FA_{native} for that participant, whereas bars that that fall to the left indicate that FA_{native} was greater than FA_{std} for that participant. Differences were plotted for each approach: A) CP Hand Drawn ROI approach, B) CP Template ROI approach, C) Probabilistic Tract, and D) Tract Template approach.

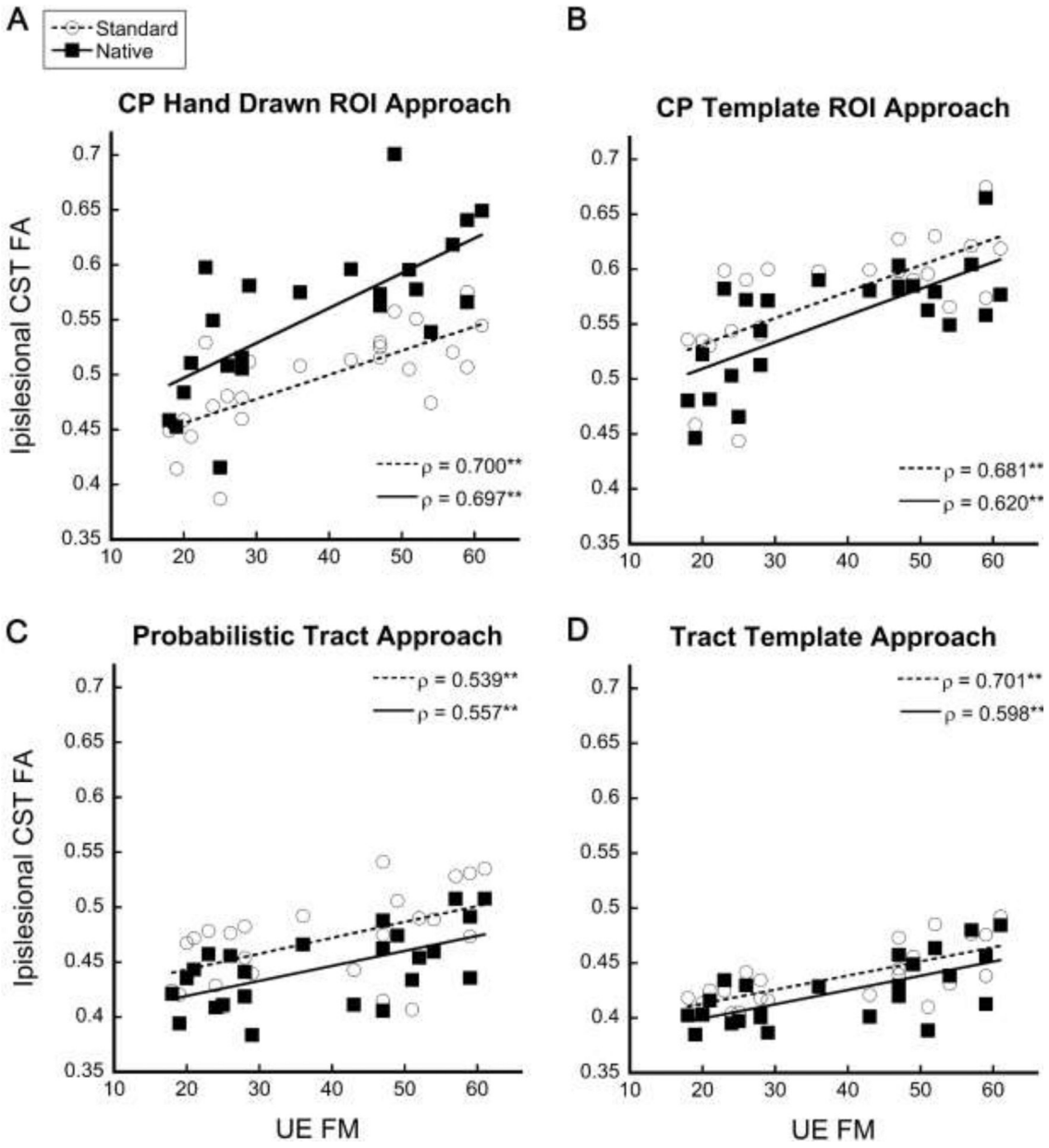

Figure 4:

Ipsilesional CST FA values from standard space and native space correlated with upper extremity impairment measured by the UE FM for each approach: A) CP Hand Drawn ROI approach, B) CP Template ROI approach, C) Probabilistic Tract, and D) Tract Template approach. CST = corticospinal tract; FA = fractional anisotropy; UE FM = Upper Extremity Fugl-Meyer; CP = Cerebral Peduncle. **Significant at p<0.0125

Table 1:

Individual participant demographics and descriptors

Subject	Sex	Age (y)	Lesion Side	Lesion Location	Lesion Volume (mm3)	Months Post Stroke	UE FM	Box and Blocks
1	M	68	L	SC	302	83	28	20/52
2	M	67	L	C/SC	113222	158	51	50/51
3	F	63	L	SC	3047	49	47	22/34
4	M	61	L	C/SC	183536	40	29	17/44
5	M	65	L	C/SC	67729	113	47	33/49
6	M	59	R	SC	1660	25	20	4/49
7	M	61	L	SC	188	41	26	13/42
8	M	40	R	CB/BS	23017	53	61	48/51
9	M	56	R	SC	14993	13	24	8/53
10	M	47	R	SC	3347	11	21	4/68
11	M	61	L	BS	199	12	52	44/55
12	M	57	L	SC	1635	6	36	28/46
13	F	53	R	C/SC	30003	13	43	23/31
14	F	67	R	SC	6170	22	28	2/43
15	F	60	R	SC	3691	7	59	44/48
16	F	35	L	BS	810	41	59	16/51
17	F	64	R	C/SC	16299	12	54	36/44
18	M	56	L	SC	1044	22	18	2/45
19	M	69	L	C/SC	105620	35	47	21/55
20	M	76	L	C/SC	30599	21	57	41/45
21	M	62	L	C/SC	174158	36	49	22/58
22	M	53	R	SC?	2673	6	25	3/52
23	M	58	L	SC	1623	8	19	3/61
24	M	72	R	C/SC	62754	6	23	10/39

y = years; C = cortical; SC = subcortical; CB = cerebellum; BS = brainstem; UE FM = Upper Extremity Fugl-Meyer, with maximum score of 66 meaning less impairment; Box and Blocks = number of blocks moved with affected hand/number of blocks moved with unaffected hand

Table 2:

Means and Difference between Standard and Native Space Values

	Mean Standard	Mean Native	Mean Difference	Mean Abs. Difference
CP Hand Drawn ROI				
FA				
Ipsilesion	0.496 *†	0.556 *†	−0.059	0.059
	(0.046)	(0.066)	(0.030)	(0.030)
Contralesion	0.550 *†	0.632 *†	−0.082	0.082
	(0.028))	(0.048))	(0.027)	(0.027)
Ratio	0.902 *	0.880 *	0.022	0.039
	(0.072)	(0.091)	(0.038)	(0.020)
Asymmetry	0.053 *	0.066 *	−0.013	0.022
	(0.041)	(0.053)	(0.022)	(0.012)
MD ($\times 10^{-3}$ mm^2/s)				
Ipsilesion	1.153 *†	1.057 *†	0.097	0.099
	(0.082)	(0.095)	(0.054)	(0.050)
Contralesion	1.076 *†	0.936 *†	0.140	0.140
	(0.057)	(0.081)	(0.047)	(0.047)
CP Template ROI				
FA				
Ipsilesion	0.576 *†	0.554 *†	0.021	0.023
	(0.052)	(0.051)	(0.017)	(0.015)
Contralesion	0.625 *†	0.600 *†	0.025	0.025
	(0.027)	(0.026)	(0.011)	(0.011)
Ratio	0.921	0.923	−0.003	0.025
	(0.072)	(0.071)	(0.032)	(0.019)
Asymmetry	0.043	0.041	0.002	0.014
	(0.041)	(0.040)	(0.018)	(0.012)
MD ($\times 10^{-3}$ mm^2/s)				
Ipsilesion	0.824	0.835	−0.011	0.018
	(0.060)	(0.061)	(0.022)	(0.016)
Contralesion	0.796 *	0.816 *	−0.020	0.022
	(0.041)	(0.044)	(0.022)	(0.020)
Probabilistic Tract				
FA				
Ipsilesion	0.470 *†	0.444 *†	0.025	0.028
	(0.041)	(0.034)	(0.018)	(0.013)
Contralesion	0.512 *†	0.479 *†	0.033	0.033
	(0.024)	(0.024)	(0.008)	(0.008)

	Mean Standard	Mean Native	Mean Difference	Mean Abs. Difference
Ratio	0.917	0.928	−0.011	0.033
	(0.057)	(0.053)	(0.040)	(0.025)
Asymmetry	0.044	0.038	0.006	0.018
	(0.031)	(0.029)	(0.022)	(0.014)
MD (×10^{-3} mm^2/s)				
Ipsilesion	0.851 †	0.849 †	0.002	0.016
	(0.078)	(0.080)	(0.022)	(0.016)
Contralesion	0.763 *†	0.773 *†	−0.010	0.010
	(0.021)	(0.021)	(0.007)	(0.007)
Tract Template				
FA				
Ipsilesion	0.437 *†	0.423 *†	0.013	0.015
	(0.027)	(0.029)	(0.011)	(0.008)
Contralesion	0.468 *†	0.457 *†	0.011	0.011
	(0.017)	(0.018)	(0.006)	(0.006)
Ratio	0.932	0.925	0.007	0.017
	(0.035)	(0.042)	(0.021)	(0.014)
Asymmetry	0.035	0.039	−0.004	0.009
	(0.019)	(0.023)	(0.012)	(0.008)
MD (×10^{-3} mm^2/s)				
Ipsilesion	0.864 *†	0.840 *†	0.025	0.025
	(0.086)	(0.069)	(0.025)	(0.024)
Contralesion	0.775 *†	0.768 *†	0.007	0.007
	(0.024)	(0.022)	(0.005)	(0.005)

*Significant difference between native and standard space value at corrected p<0.0125

†Significant difference between ipsilesional and contralesional value at corrected p<0.0125

Table 3:

Correlations between CST FA and Arm Motor Impairment and Arm Function

	CP Hand Drawn ROI		CP Template ROI		Probabilistic Tract		Tract Template	
	Std	**Nat**	**Std**	**Nat**	**Std**	**Nat**	**Std**	**Nat**
UE FM								
FA								
Ipsilesion	0.700 *	0.697 *	0.681 *	0.620 *	0.539 *	0.557 *	0.701 *	0.598 *
Ratio	0.607 *	0.691 *	0.621 *	0.566 *	0.602 *	0.488	0.588 *	0.463
Asymmetry	−0.607 *	−0.691 *	−0.621 *	−0.566 *	−0.602 *	−0.488	−0.588	−0.463
ARAT								
FA								
Ipsilesion	0.627 *	0.621 *	0.672 *	0.562 *	0.384	0.434	0.592 *	0.512 *
Ratio	0.549 *	0.656 *	0.620 *	0.540 *	0.429	0.397	0.468	0.414
Asymmetry	−0.549 *	−0.656 *	−0.620 *	−0.540 *	−0.429	−0.397	−0.468	−0.414

UE FM=Upper Extremity Fugl-Meyer; ARAT=Action Research Arm Test. All values are Spearman's rho.

*Significant correlation at corrected p<0.0125